Wave Cancellation Properties of a Splitter-Plate Porous Wall Configuration

G. M. Elfstrom*
DSMA International, Inc., Toronto, Canada
B. Medved†
Vazduhoplovnotehnički Institut, Belgrade, Yugoslavia
and
W. J. Rainbird‡
Carleton University, Ottawa, Canada

The wave cancellation properties of an inclined-hole porous wall are examined for the case where each hole has a splitter plate designed for edgetone noise attenuation. Wave cancellation is ascertained by comparing measured cone/cylinder surface pressure signatures with those measured in the very low blockage tests carried out in the Arnold Engineering Development Center (AEDC) 16-ft wind tunnel, for a range of wall porosity settings, over a Mach number range of 1.0–1.4. In general, the present data show that low wall interference can be obtained. The optimum porosity settings are distinctly lower than those found for the AEDC 4-ft wind tunnel.

Nomenclature

BOF	= mass fraction of air blown off, %
C_p	= pressure coefficient, $=(p-p_\infty)/q_\infty$
D	= model cylinder diameter
m	= Mach number
p	= pressure
q	= dynamic pressure
X	= distance along model centerline from nose
τ	= test-section wall porosity, %

Subscripts

n	= nominal conditions
ref	= conditions measured at a reference point
w	= conditions at test-section wall
0	= stagnation conditions
∞	= freestream static conditions (calibrated)

Introduction

THE Vazduhoplovnotehnički Institut (VTI) trisonic blowdown wind tunnel[1] has a transonic test section with two- and three-dimensional inserts. The inserts have inclined-hole porous walls with variable porosity adjustment capability. To alleviate the edgetone noise generated by the holes in the wall, splitter plates[2] were incorporated into the hole design. The question naturally arises as to the effect of the splitter plates on the crossflow characteristics of each hole, i.e., on the wall interference properties. The study described in the present paper was carried out to determine if there was any significant influence on the wall interference properties and then to find the optimum wall porosity settings for the three-dimensional insert case. The study emphasized wave cancellation properties in the upper transonic speed range; however, some investigation was made into solid blockage aspects at subsonic speeds.

Facility Description

The wind tunnel has a transonic test section that can be installed in tandem within the circuit. Mach number is nominally set using either the second throat or flexible nozzle contour, depending on whether the flow is to be subsonic or supersonic. Final Mach number trimming is done using a blowoff system (with ejector assist if required) in which air reenters the circuit in the wide-angle diffuser just before the exhaust stack. Figure 1 shows a schematic of the circuit airline.

Each of the four parallel walls of the three-dimensional insert are 1.5-m wide by 4.6-m long, of which 0.6 m extends into the model cart. Each wall consists of a pair of perforated plates with holes inclined 60 deg to the vertical. Variable porosity is achieved by sliding the backplate to throttle the hole openings, the range being 1.5–8%. Motion of the throttle plate is forward from full-open; i.e., cutoff is from the downstream edge of each hole.

A hole size of 12.8 mm was chosen to meet the flow quality requirements in accordance with the method of Goethert,[3] and to avoid problems associated with large diameter/boundary-layer displacement thickness ratios. In addition, as recommended by Goethert, the plate thickness was made as close to the hole diameter as stiffness concerns would allow. The combined two-plate thickness was 14 mm. A splitter plate 2-mm thick is integral with each hole in the main plate—splitters are not incorporated into the throttle plate. As a safeguard against plenum pumping action through pressure communication in the axial direction, the distance between successive holes was maximized by slewing the hole pattern. Figure 2 shows the hole geometry and "finger" region where the porosity is gradually developed on a wall. A reference static hole ("ref." in Fig. 2) located on one wall is used for control of nominal Mach number during a test run.

For each second throat or flexible nozzle setting, a range of Mach numbers is possible using the blowoff system. Figure 3 shows a plot of the Mach number obtained from the test-section sidewall reference pressure measurement for various blowoff mass fractions and nominal Mach numbers based on the second throat or flexible nozzle settings. The lines denoted "range of BOF used" represent only part of the BOF range

Presented as Paper 88-2003 at the AIAA 15th Aerodynamic Testing Conference, San Diego, CA, May 18–20, 1988; received Aug. 6, 1988; revision received March 10, 1989. Copyright © 1988 American Institute of Aeronautics and Astronautics, Inc. All rights reserved.

*Chief Aerodynamicist. Member AIAA.
†Head, High Speed Aero Department. Presently, Senior Research Engineer, Lola Institut, Belgrade, Yugoslavia.
‡Professor (retired), Department of Mechanical Engineering. Member AIAA.

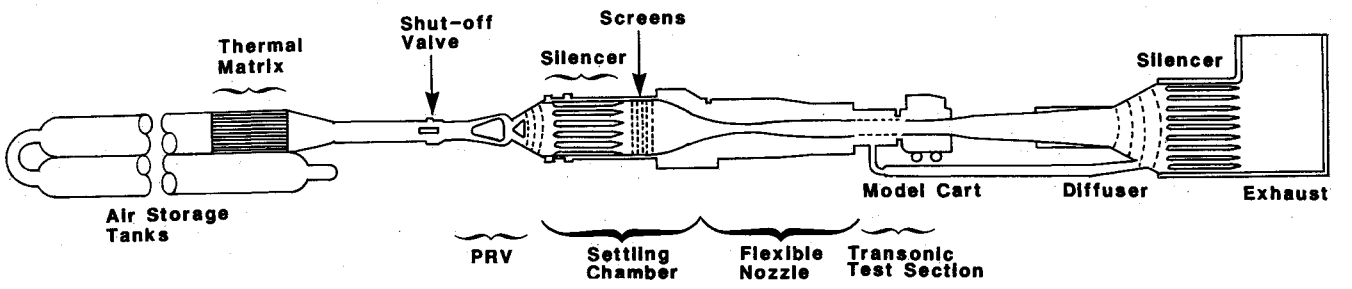

Fig. 1 Schematic of wind tunnel (PRV = pressure regulating valve).

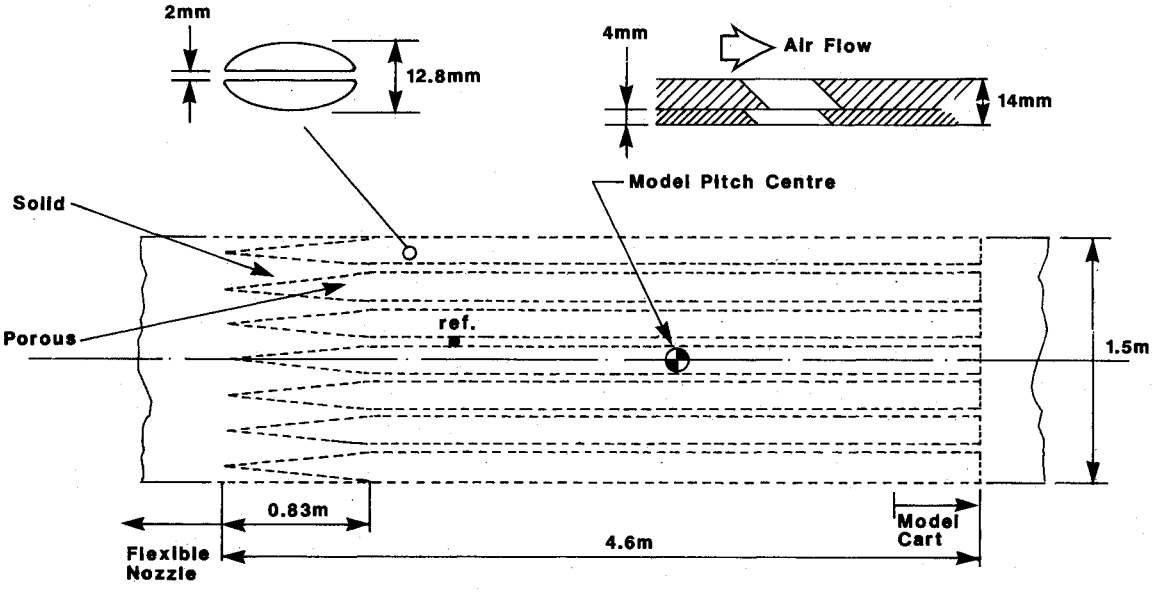

Fig. 2 Schematic of test-section walls.

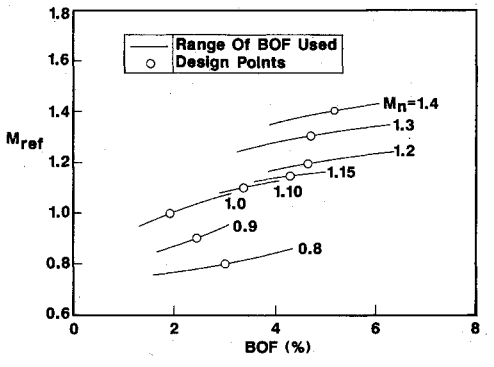

Fig. 3 Use of blowoff to trim Mach number.

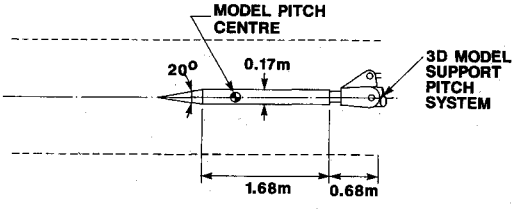

Fig. 4 Cone/cylinder model in transonic test section.

achievable at each nominal Mach number. The specific ranges were chosen with two criteria in mind: 1) to enable overlap from one nominal setting to another, and 2) to maintain enough blowoff to compensate for boundary-layer growth over the "rough" test-section wall.

The equivalent freestream Mach number was obtained from a calibration of the reference hole against a centerline probe.

Test Model and Procedure

The test model used was a 1% blockage cone/cylinder shape, consisting of a 10-deg half-angle sharp cone followed by a cylinder 10 diam long. Total model length was approximately 2.16 m. Surface static pressures were sensed by 42 0.7-mm orifices, of which 36 were along one generator. All orifices were connected to a D9 Scanivalve with a 1-bar Druck pressure transducer referenced to the test-section sidewall static pressure. The model was mounted off the main model sting support strut, with the sting and roll drive removed. A layout showing the model geometry and its location in the transonic test section is presented in Fig. 4. Test-section sidewall static pressures were sensed simultaneously with the cone/cylinder pressures using 1.4-mm-diam orifices located on a line running through the reference static hole.

Tests were conducted at Mach numbers between 0.6 and 1.4, at blowing pressure and wall porosity settings as indicated in Table 1. Total temperature was generally room temperature (22°C), so that Reynolds number based on model diameter was high, e.g., 7.7×10^6 at $M_\infty = 1.0$. For all tests, the model was held aligned with the flow, i.e., at zero pitch and yaw angles.

Results

Data Checks

A repeatability test at $M_\infty = 1.05$ revealed cone × cylinder surface pressures to be within ± 0.001 on a basis of p/p_0. The corresponding sidewall pressure repeatability was ± 0.002 on a basis of C_p.

Wall pressure signatures were examined for influence of the model flowfield on the sidewall reference static pressure measurement, particularly at high subsonic speeds. This was done by comparing empty test-section signatures with those where

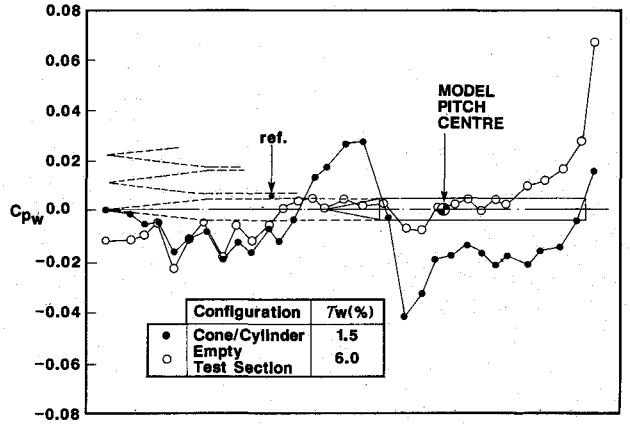

Fig. 5 Upper wall pressure signatures, $M_\infty = 0.975$.

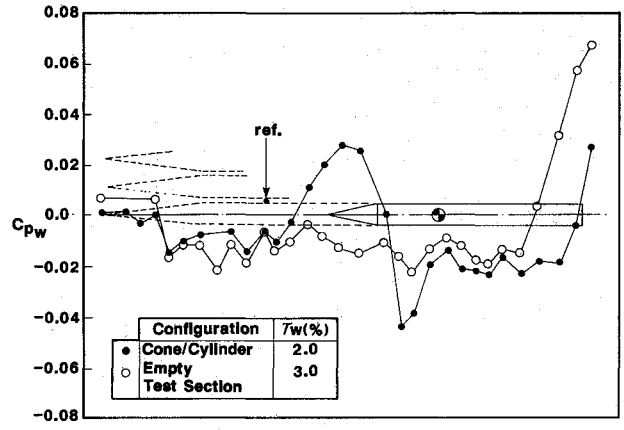

Fig. 6 Upper wall pressure signatures, $M_\infty = 1.0$.

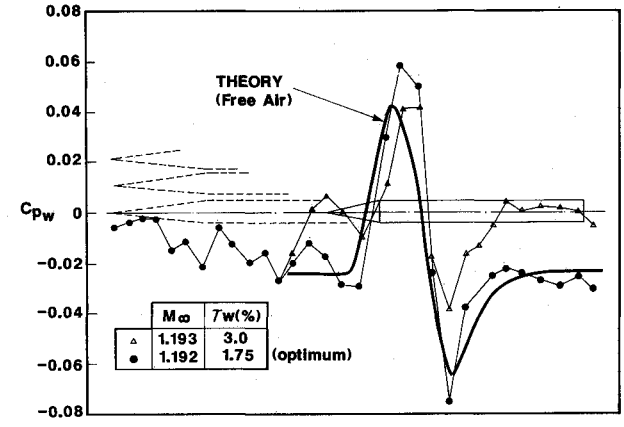

Fig. 7 Upper wall pressure signatures, $M_\infty = 1.2$.

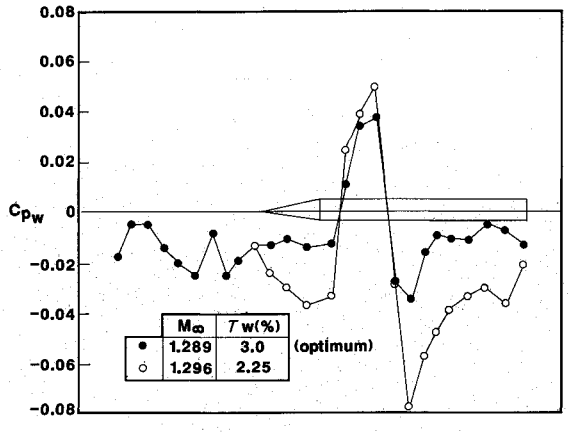

Fig. 8 Upper wall pressure signatures, $M_\infty = 1.3$

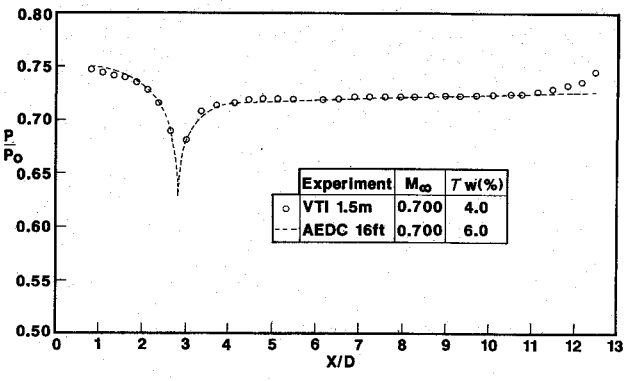

Fig. 9 Cone/cylinder pressure distribution, $M_\infty = 0.7$.

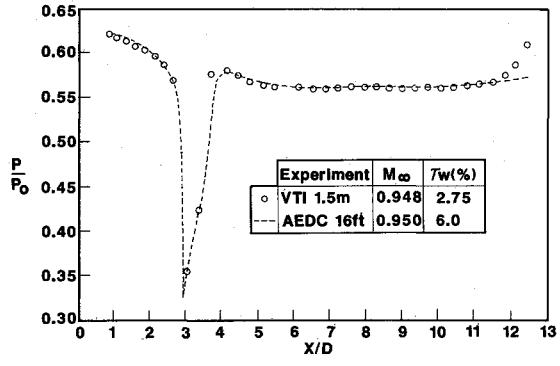

Fig. 10 Cone/cylinder pressure distribution, $M_\infty = 0.95$.

the cone/cylinder model was present. Results showed that the pressure rise associated with the stagnation region of the model begins slightly downstream of the reference hole, as indicated in Fig. 5, for example. The pressure rise seen near the downstream end of the model is most likely due to the influence of the model support pitch system (see Fig. 4). This pressure rise is located beyond the region normally occupied by an aircraft model and, thus, is of no concern.

Calibration tests in the empty test section and, hence, early tests in this program were conducted with porosity settings according to the recommendation for the Arnold Engineering Development Center (AEDC) 4-ft wind tunnel.[4] However, these settings were found to be very inappropriate insofar as shock cancellation properties were concerned. Much lower porosity settings were required, as discussed later. This is the reason for the mismatch of porosity levels indicated in Fig. 5. Wall pressure signatures for nearly matched porosity settings are shown in Fig. 6. Note that there is only a slight variation in wall pressure along the porosity development region. This indicates that the blowoff fraction (BOF in Fig. 3) is about optimum, i.e., just sufficient to account for boundary-layer growth.

Wall Static Pressure Distribution

Selection of optimum wall porosity settings was corroborated by wall static pressure signatures. In addition to those shown in Figs. 5 and 6, typical distributions are also given in Figs. 7 and 8. Discussion of these signatures is given later.

Cone/Cylinder Surface Static Pressure Distributions

Representative cone/cylinder pressure signatures are shown in Figs. 9–14. For reference, the corresponding pressure distributions from a low blockage (0.063%) model test carried out

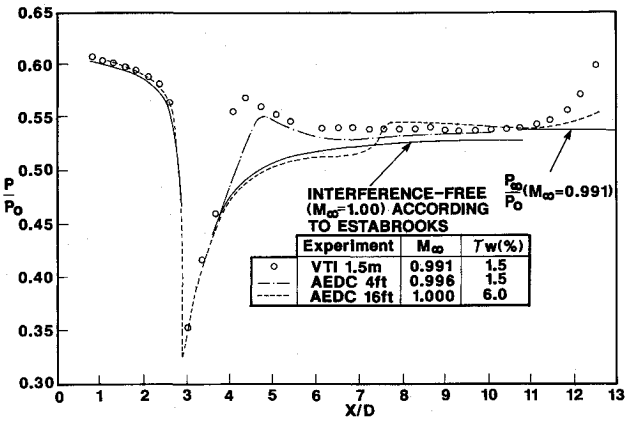

Fig. 11 Cone/cylinder pressure distribution, $M_\infty = 1.0$.

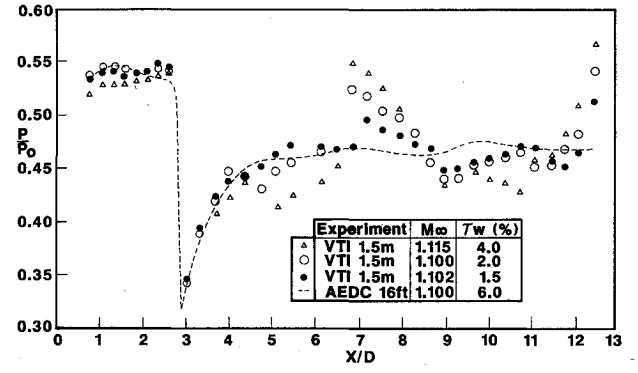

Fig. 12 Cone/cylinder pressure distribution, $M_\infty = 1.1$.

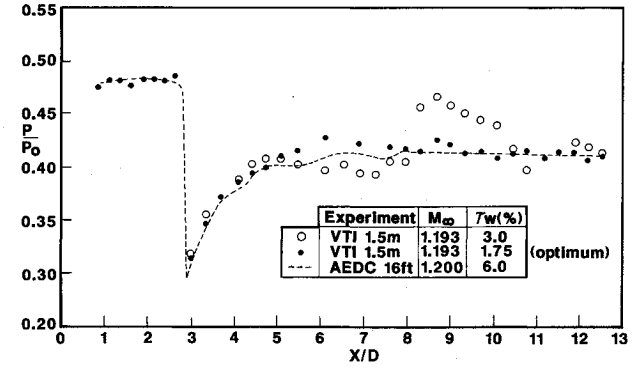

Fig. 13 Cone/cylinder pressure distribution, $M_\infty = 1.2$.

in the AEDC 16-ft wind tunnel[5] are also shown in the figures. The pressure field associated with the model support pitch system can be seen in the aft region of the cylinder pressure distributions.

Discussion

Wall Interference Assessment

The best agreement with the AEDC reference data occurred at relatively low porosity settings, in contrast to those expected from the AEDC 4-ft wind-tunnel tests, particularly at the higher Mach numbers. For example, consider the $M_\infty = 1.1$ case (Fig.12). Here it can be seen that, near the AEDC 4-ft optimum level (2.5%), the wall is too "open"; i.e, the bow shock reflects onto the model as an expansion wave, while the expansion wave emanating from the cone/cylinder junction reflects onto the model as a shock wave. The data suggest that a slight improvement in shock/expansion cancellation properties might be obtained if a porosity setting less than the lowest achievable (1.5%) were possible.

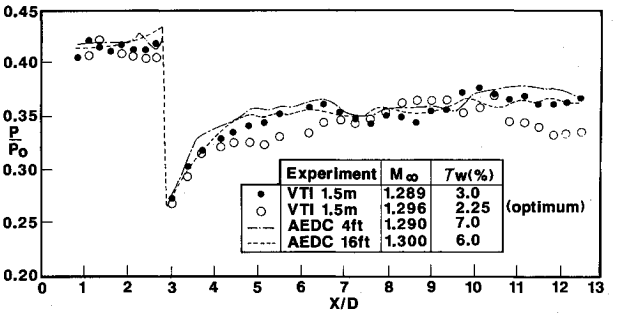

Fig. 14 Cone/cylinder pressure distribution, $M_\infty = 1.3$.

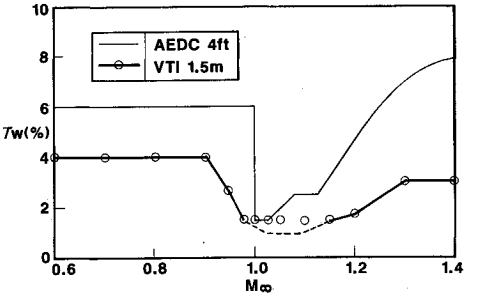

Fig. 15 Optimum porosity settings.

Table 1 Summary of test conditions

M_∞	p_0, bar	τ_w, %
0.6	2.0	4.0
0.7	3.0	4.0
0.8	3.0	4.0
0.9	3.0	4.0
0.95	3.0	2.75
0.975	3.0	1.5
1.00	3.0	1.5, 2.0
1.025	3.0	1.5, 2.0
1.05	3.0	1.5, 2.0
1.1	3.0	1.5, 2.0, 3.0, 4.0
1.15	3.0	1.5
1.2	3.0	1.5, 1.75, 2.25, 3.0
1.3	4.0	2.25, 3.0, 3.5
1.4	4.0	3.0, 3.5, 4.5

Porosity settings that produce the best agreement with the AEDC 16-ft wind-tunnel test results show the most logical wall pressure signatures. For example, consider the $M_\infty = 1.2$ case (Fig. 7). When the porosity setting is too high, there is a precursor pressure rise ahead of the shock impingement rise and an overall rise downstream. The signature associated with the optimum porosity shows no precursor and a return to a level close to the undisturbed value. The exact opposite occurs when the porosity setting is too low, as seen in Fig. 8. A free-air prediction[6] of the static pressure signature along a line located at a position equivalent to the test-section wall was made for the $M_\infty = 1.192$ case; the results are plotted in Fig. 7. Although caution must be taken[7] when comparing predictions with experiments, the agreement does suggest that approximately the correct pressure distribution is measured for the far-field perturbation due to the shock/expansion flowfield. This is further evidence that optimum wave cancellation has been achieved.

The case of $M_\infty = 1.0$ is quite interesting. The cone/cylinder pressure distribution (Fig. 11) for the AEDC reference data indicates that the walls are too open, in spite of the low blockage level (0.063%). In comparison, both the present data and those from the 4-ft wind-tunnel tests[4] show, if anything, a weak, but opposite, effect. The question to be raised is: What constitutes "interference-free" results? The data often referenced as such are those due to Estabrooks,[8] quoted in the

report[4] for the AEDC 4-ft results. The present data show a much quicker recovery to the freestream (undisturbed) level on the cylinder, as does the wall static pressure (Fig. 6). Tests with a smaller blockage model, including lower porosity settings, are needed to resolve this issue.

Cone/cylinder data at subsonic speeds, e.g., Figs. 9 and 10, agree very closely with the AEDC 16-ft data. Since the wall static pressure distributions show a recovery to undisturbed levels in the region of the cylinder (e.g., Fig. 5), the present porosity settings should provide low wall interference, in particular low solid blockage effects. Note, however, that settings other than the values shown in Table 1 have not been tested to date. In addition, the present experiment did not address other aspects of subsonic wall interference, such as induced flow angularity in the case of lifting models.

Optimum Porosity Schedule

A plot of the optimum porosity settings found in the present study is given in Fig. 15, along with the recommended schedule[4] for the AEDC 4-ft wind tunnel. The cone/cylinder pressure distributions suggest that between $M_\infty = 1.0$ and 1.1 porosity levels less than the lowest achievable (1.5%) would effect some improvement. The broken line shown in Fig. 15 is a recommended schedule based on extrapolations of results such as those given in Fig. 12.

Since the time of the cone/cylinder tests in the AEDC 4-ft wind tunnel, other facilities with 60-deg inclined-hole porous walls have also reported low optimum porosity settings. For example, Lockheed-Georgia[9] has found that a porosity of about 3.5% is generally optimum for testing in the range $M = 0.2$–0.95 in the three-dimensional test section of their 20×28-in. wind tunnel, which has a porous wall design almost identical to that of the AEDC 4-ft wind tunnel. Minimal blockage corrections have been obtained with porosities between 2.5 and 4.0% in two-dimensional model tests[10] carried out in the Lockheed wind tunnel. It is interesting to note that Grunnet[11] advocates near-closure of the porous wall close to sonic conditions.

The optimum porosities found in the present study may be peculiar to the VTI facility, since they appear somewhat at odds with other reported results. Alternatively, the wall boundary-layer responsiveness to crossflow may be altered slightly by the presence of splitter plates. A detailed experimental investigation into this subject is required to resolve the issue.

The chief benefit of cone/cylinder tests is to establish porosity settings that effect optimum shock/expansion cancellation at the wall under supersonic test conditions. The present tests have shown that this is achievable using a wall design that incorporates splitter plates integral with porous wall holes. Concerning subsonic wall interference minimization, the wall pressure signatures demonstrate that solid blockage compensation is achievable.

Conclusions

Experiments carried out using a 1% blockage cone/cylinder model in the three-dimensional transonic test section of the Vazduhoplovnotehnički Institut 1.5-m blowdown wind tunnel have shown that minimal wall interference can be achieved when 60-deg inclined-hole porous walls are fitted with splitter plates. Optimum porosity settings in the supersonic range were found to be significantly lower than those suggested for the Arnold Engineering Development Center 4-ft wind tunnel. It is reasonable to conclude that there is nothing unique about the presence of splitter plates in porous wall holes.

Acknowledgment

The authors would like to thank D. J. Jones of the High Speed Aerodynamics Laboratory at the National Aeronautical Establishment, Ottawa, for running RAXBOD, the program that produced the $M_\infty = 1.2$ free-air predictions.

References

[1]Medved, B. and Elfstrom, G. M., "The Yugoslav 1.5 m Trisonic Blowdown Wind Tunnel," AIAA Paper 86-0746, 1986.

[2]Dougherty, N. S., Anderson, C. F., and Parker, R. L., "An Experimental Study on Suppression of Edgetones from Perforated Wind Tunnel Walls," AIAA Paper 76-50, 1976.

[3]Goethert, B. H., *Transonic Wind Tunnel Testing,* Pergamon, New York, 1961, p. 279.

[4]Jacocks, J. L., "Determination of Optimum Operating Parameters for the AEDC-PWT 4 ft Transonic Tunnel with Variable Porosity Test Section Walls," Rept. AEDC-TR-69-164, Arnold Engineering Development Center, Tullahoma, TN, Aug. 1969.

[5]Hartley, M. S. and Jacocks, J. L., "Static Pressure Distributions on Various Bodies of Revolution at Mach Numbers from 0.60 to 1.60," Rept. AEDC-TR-68-37, Arnold Engineering Development Center, Tullahoma, TN, March 1968.

[6]South, J. C., Jr. and Jameson, A., "Relaxation Solutions for Inviscid Axisymmetric Transonic Flow Over Blunt or Pointed Bodies," *Proceedings of the AIAA Computational Fluid Dynamics Conference,* July 1973, pp. 8–17.

[7]Nyberg, S.-E. and Sorenson, H., "Experimental Investigation of the Interference-Free Flowfield Around a Lifting Body Model to Establish Cross Flow Characteristics for Ventilated Wind Tunnel Walls at Low Supersonic Mach Numbers," AIAA Paper 80-0444, 1980.

[8]Estabrooks, B. B., "Wall Interference Effects on Axisymmetric Bodies in Transonic Wind Tunnels," Rept. AEDC-TR-59-12, Arnold Engineering Development Center, Tullahoma, TN, June 1959.

[9]Pounds, G. A., private communication, July 1986.

[10]Blackwell, J. A., "Wind Tunnel Blockage Correction for Two-Dimensional Transonic Flow," *Journal of Aircraft,* Vol. 16, April 1979, pp. 256–263.

[11]Grunnet, J. L., "Transonic Wind Tunnel Wall Interference Minimization," *Journal of Aircraft,* Vol. 21, Sept. 1984, pp. 694–699.